

retrospectively based on near-daily records of swelling size and state. Observers recorded all agonistic interactions and interventions on an *ad libitum* basis. In each case of agonism, observers recorded the identity of individuals involved in the aggressive encounter and its outcome³⁰. When third parties intervened in disputes, observers recorded the identity of the individual who intervened (ally), the identity of the individual that received support, the identity of the individual against whom support was directed, and the type of support that was provided. Support took two forms. Allies either directed overt aggression towards one of the participants (designated the opponent), or established close proximity or affiliative physical contact with one of the participants (designated the beneficiary). See ref. 31 for more details of data collection; methods employed in that study were identical to those employed here.

Adult males supported juveniles in 193 disputes. In 93 of these events, both disputants were juveniles (less than 4 years old); in 36, the opponent was an adult female; in 49, a subadult male; and in 15, an adult male (see ref. 27 for definitions of subadult and adult males). The median age of juvenile recipients of adult male help was 2.25 yr; the interquartile range was 1.75 yr to 3.13 yr, and the youngest recipient was 4 months old.

Received 15 April; accepted 30 June 2003; doi:10.1038/nature01866.

1. Woodroffe, R. & Vincent, A. Mother's little helpers: patterns of male care in mammals. *Trends Ecol. Evol.* **9**, 294–297 (1994).
2. Smuts, B. B. & Gubernick, D. J. in *Father–Child Relations* (ed. Hewlett, B. S.) 1–30 (Aldine De Gruyter, New York, 1992).
3. van Schaik, C. P. & Paul, A. Male care in primates: does it ever reflect paternity? *Evol. Anthropol.* **5**, 152–156 (1996).
4. Trivers, R. L. in *Sexual Selection and the Descent of Man 1871–1971* (ed. Campbell, B.) (Aldine, Chicago, 1972).
5. Borries, C., Launhardt, K., Epplen, C., Epplen, J. T. & Winkler, P. Males as infant protectors in Hanuman langurs (*Presbytis entellus*) living in multimale groups—defence pattern, paternity and sexual behaviour. *Behav. Ecol. Sociobiol.* **46**, 350–356 (1999).
6. Paul, A., Kuester, J. & Arnemann, J. The sociobiology of male–infant interactions in Barbary macaques. *Macaca sylvanus. Anim. Behav.* **51**, 155–170 (1996).
7. Ménard, N. *et al.* Is male–infant caretaking related to paternity and/or mating activities in wild Barbary macaques (*Macaca sylvanus*)? *C.R. Acad. Sci. III Vie* **324**, 601–610 (2001).
8. Altmann, J. *et al.* Behavior predicts genetic structure in a wild primate group. *Proc. Natl Acad. Sci. USA* **93**, 5797–5801 (1996).
9. Sherman, P. W., Reeve, H. K. & Pfennig, D. W. in *Behavioural Ecology: An Evolutionary Approach* (eds Krebs, J. R. & Davies, N. B.) 69–96 (Blackwell Scientific, Oxford, 1997).
10. Hauber, M. E. & Sherman, P. W. Self-referent phenotype matching: theoretical considerations and empirical evidence. *Trends Neurosci.* **24**, 609–616 (2001).
11. Singh, D. & Bronstad, P. Female body odour is a potential cue to ovulation. *Proc. R. Soc. Lond. B* **268**, 797–801 (2001).
12. Wedekind, C., Seebeck, T., Bettens, F. & Paepke, A. J. MHC-dependent mate preferences in humans. *Proc. R. Soc. Lond. B* **260**, 245–249 (1995).
13. Wedekind, C. & Furi, S. Body odour preferences in men and women: do they aim for specific MHC combinations or simply heterozygosity? *Proc. R. Soc. Lond. B* **264**, 1471–1479 (1996).
14. Ober, C. *et al.* HLA and mate choice in humans. *Am. J. Hum. Genet.* **61**, 497–504 (1997).
15. Jacob, S., McClintock, M. K., Zelano, B. & Ober, C. Paternally inherited HLA alleles are associated with women's choice of male odours. *Nature Genet.* **30**, 175–179 (2002).
16. Halpin, Z. T. in *Kin Recognition* (ed. Hepper, P. G.) 220–258 (Cambridge Univ. Press, Cambridge, 1991).
17. Parr, L. A. & de Waal, F. B. M. Visual kin recognition in chimpanzees. *Nature* **399**, 647–648 (1999).
18. Widdig, A., Nürnberg, P., Krawczak, M. & Bergovitch, F. B. Paternal relatedness and age proximity regulate social relationships among adult female rhesus macaques. *Proc. Natl Acad. Sci. USA* **98**, 13769–13773 (2001).
19. Smith, K., Alberts, S. C. & Altmann, J. Wild female baboons bias their social behaviour towards paternal half-sisters. *Proc. R. Soc. Lond. B* **270**, 503–510 (2003).
20. Alberts, S. C. Paternal kin discrimination in wild baboons. *Proc. R. Soc. Lond. B* **266**, 1501–1506 (1999).
21. Soltis, J., Thomsen, R., Matsubayashi, K. & Takenaka, O. Infanticide by resident males and female counter-strategies in wild Japanese macaques (*Macaca fuscata*). *Behav. Ecol. Sociobiol.* **48**, 195–202 (2000).
22. Silk, J. B. Kin selection in primate groups. *Int. J. Primatol.* **23**, 849–875 (2002).
23. Palombit, R. A., Seyfarth, R. M. & Cheney, D. L. The adaptive value of 'friendships' to female baboons: experimental and observational evidence. *Anim. Behav.* **54**, 599–614 (1997).
24. Smith, K. L. *et al.* Cross-species amplification, non-invasive genotyping, and non-mendelian inheritance of human STRPs in savannah baboons. *Am. J. Primatol.* **51**, 219–227 (2000).
25. Morin, P. A., Chambers, K. E., Boesch, C. & Vigilant, L. Quantitative polymerase chain reaction analysis of DNA from noninvasive samples for accurate microsatellite genotyping of wild chimpanzees (*Pan troglodytes verus*). *Mol. Ecol.* **10**, 1835–1844 (2001).
26. Taberlet, P. *et al.* Reliable genotyping of samples with very low DNA quantities using PCR. *Nucleic Acids Res.* **24**, 3189–3194 (1996).
27. Alberts, S. C. & Altmann, J. Preparation and activation: determinants of age at reproductive maturity in male baboons. *Behav. Ecol. Sociobiol.* **36**, 397–406 (1995).
28. Marshall, T. C., Slate, J., Kruuk, L. E. B. & Pemberton, J. M. Statistical confidence for likelihood-based paternity inference in natural populations. *Mol. Ecol.* **7**, 639–655 (1998).
29. Shaikh, A. A., Celaya, C. L., Gomez, I. & Shaikh, S. A. Temporal relationship of hormonal peaks to ovulation and sex skin deturgescence in the baboon. *Primates* **23**, 444–452 (1982).
30. Hausfater, G. *Dominance and Reproduction in Baboons (Papio cynocephalus)* (Basel, Karger, 1975).
31. Silk, J. B., Alberts, S. C. & Altmann, J. Patterns of coalition formation by adult female baboons in Amboseli, Kenya. *Anim. Behav.* (in the press).

Acknowledgements We thank the Office of the President of the Republic of Kenya and the Kenya Wildlife Service for permission to work in Amboseli, and the Institute of Primate Research for local sponsorship. We also thank the Wardens and staff of Amboseli National Park, and the pastoralist communities of Amboseli and Longido for continuous cooperation and assistance. We acknowledge financial support from the National Science Foundation (to J.A., J.B.S. and S.C.A.), the Chicago Zoological Society (to J.A.), the L.S.B. Leakey Foundation and the National Geographic Society (J.B.S.). We thank M. Lavine, of the Duke University Statistical Consulting Center, and R. Zimmerman for advice and assistance with statistical tests; R. S. Mututua, S. N. Sayialel and J. K. Warutere for data and sample collection. C. Packer and R. Palombit provided comments on the manuscript.

Competing interests statement The authors declare that they have no competing financial interests.

Correspondence and requests for materials should be addressed to S.C.A. (alberts@duke.edu).

Motion-induced spatial conflict

Derek H. Arnold & Alan Johnston

Department of Psychology and Institute of Cognitive Neuroscience, University College London, Gower Street, London WC1E 6BT, UK

Borders defined by small changes in brightness (luminance contrast) or by differences in colour (chromatic contrast) appear to move more slowly than those defined by strong luminance contrast^{1–4}. As spatial coding is influenced by motion^{5–7}, if placed in close proximity, the different types of moving border might appear to drift apart⁸. Using this configuration, we show here that observers instead report a clear illusory spatial jitter of the low-luminance-contrast boundary. This visible interaction between motion and spatial-position coding occurred at a characteristic rate (~22.3 Hz), although the stimulus motion was continuous and invariant. The jitter rate did not vary with the speed of movement. The jitter was not due to small involuntary movements of the eyes, because it only occurred at a specific point within the stimulus, the low-luminance-contrast boundary. These findings show that the human visual system contains a neural mechanism that periodically resolves the spatial conflict created by adjacent moving borders that have the same physical but different perceptual speeds.

A bright red dot moving against a dark background provides a strong luminance-defined motion signal. A smaller equiluminant green dot superimposed on this target provides a weaker motion signal at the chromatic boundary. To the extent that motion influences spatial position^{5–7}, the green dot might be expected to lag progressively behind. This scheme has recently been suggested as an explanation for the classical 'fluttering hearts' illusion⁸ (Fig. 1).

When we created this configuration (Fig. 2a), it was clear that the two parts of the stimulus did not appear to drift apart. However, a vivid perceptual illusion was immediately apparent. When fixation was maintained on a stationary target, the spatial position of the green dot appeared to jitter while moving. To examine this phenomenon, we constructed a stimulus consisting of four dots (Fig. 2a). A small green dot was superimposed on a larger red dot to form a bull's-eye configuration. Another green dot, of the same size, was shown against a dark background (isolated motion). All these dots rotated about a central static fixation point at a constant retinal velocity of 6.75° s⁻¹. During a run of trials, we systematically manipulated the luminance of the green dots. On each trial, observers were required to indicate whether the foreground green dot or, in different trial runs, the isolated green dot appeared to jitter while moving. Jitter was reported most often when there was little or no luminance contrast between the moving foreground and back-

ground components (Fig. 3). None of our observers ever saw jitter in the isolated-motion condition.

To determine whether the perceived jitter is a general property of equiluminant motion, we presented a rotating green dot against a static red ring (Fig. 2b). By varying the luminance of the green dot, in separate trials, we could test for positional jitter at a range of luminance contrasts spanning the equiluminant point. None of our observers reported jitter for any luminance difference between the green dot and the background (Fig. 3). As jitter does not occur for isolated low-luminance-contrast motion, it is clear that the illusory jitter requires an interaction between signals generated by high and low luminance contrast (or chromatic borders). Because the effect is not generated by chromatic equiluminant motion *per se*, the illusory jitter cannot be caused by a difference in the speed with which the visual system responds to different colours⁹, or by inhibitory interactions between rod- and cone-mediated signals at the colour boundary¹⁰. In any case, although processing delays may introduce a perceptual lag, they cannot provide a sufficient explanation for positional jitter (Fig. 1).

If a difference in perceived speed between low- and high-luminance-contrast boundaries is the critical determining factor, rather than some distinguishing feature of colour processing, then jitter should also be visible for achromatic borders. We constructed a stimulus that contained two green squares presented 2° above and below a central static fixation point (Fig. 2c). The luminance of a central region within the squares was either incremented or decremented from trial to trial to generate a low-luminance-contrast boundary. The squares moved in counter-phase from left to right at a retinal velocity of 4.6° s⁻¹ with a periodicity of 0.5 Hz. Observers reported illusory jitter only when there was a small luminance contrast between the foreground and background regions of the target (Fig. 3).

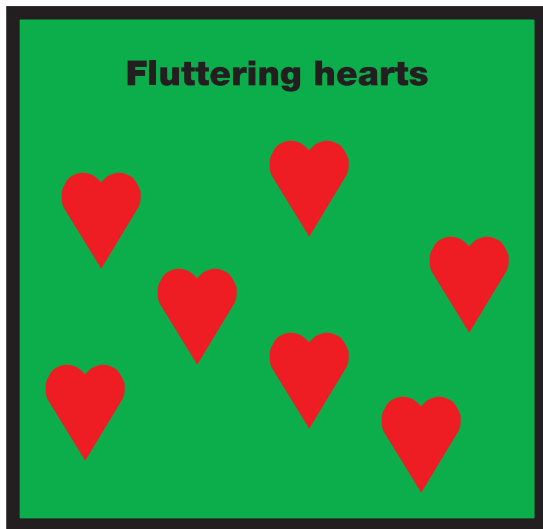


Figure 1 'Fluttering hearts' illusion. If you shake this page from side to side, the red hearts may seem to shift in position relative to the black frame. The figure combines borders of high (dark frame and surround) and low (red hearts and surround) luminance contrast. Originally, the illusion was thought to reflect differences in the speed of visual processing for different colours^{9,10}. More recently, the illusion has been attributed to a difference in the perceived speeds of the two types of moving border⁸. If the stimulus motion is kept constant, in the absence of a compensatory mechanism, the first hypothesis posits that the perceived positions of the hearts should lag that of the frame by a fixed interval. The more recent hypothesis suggests that the borders should drift apart. Here, using a configuration containing adjacent high- and low-luminance-contrast borders, we show that the low-contrast border appears to jitter. This is consistent with a corrective process that periodically snaps the perceptually slower-moving border back into spatial alignment with the faster-moving border (see Supplementary Information for demonstrations).

The illusory jitter could result from small eye movements that are present even during target fixation^{11–13}. To investigate this, we used two further configurations. In one, observers tracked the centre of the bull's-eye as it rotated (Fig. 2d). In this situation, none of the observers ever reported illusory jitter (Fig. 3). In the second, observers tracked a rotating fixation point that had the same speed and eccentricity as the target in the preceding stimulus configurations. A static red–green bull's-eye replaced the fixation point (Fig. 2e). Again, on different trials, we systematically manipulated the luminance of the central green dot while we kept the luminance of the red background dot constant. In this condition, robust illusory jitter of the foreground dot was clearly visible (Fig. 3).

These findings show that the illusory jitter is dependent on retinal and not physical motion of the bull's-eye. When the retinal position of the bull's-eye is kept relatively constant, by tracking (Fig. 2d), there is no illusory jitter (Fig. 3). We also found that there is no illusory jitter of an extrafoveal bull's-eye that moves in phase with a tracked bull's-eye target, demonstrating that the elimination of jitter for tracked targets is not simply a result of foveation.

Adding an eye-velocity vector, extracted from a copy of the motor commands or from proprioceptive extra-retinal signals, to retinal velocities while tracking could stabilize the position of static patterns^{11–13}. However, as this signal would provide a universal image compensation, it should affect all borders equally and could not explain the spatially specific positional jitter of the static bull's-eye (Fig. 2e). During informal observations, we have also found that illusory jitter can be seen when the stimulus is viewed monocularly through a pin-hole, ruling out accommodative micro-fluctuations¹⁴ as a causal mechanism, and when presentation is restricted to just 100 ms, a time span that is too short to allow saccadic movements of the eye.

Illusory jitter in a static pattern has been reported after adaptation to physical jitter in an adjacent part of the visual field^{15–16}. This illusion has been taken as evidence for a mechanism that stabilizes the visual image by calculating a baseline velocity from the region of the retina that has the lowest instantaneous velocity, and subtracting this baseline from all image velocities^{15–16}. The illusory jitter reported here differs from the jitter after-effect because the after-effect results in synchronous jitter for all non-adapted locations, whereas the illusory jitter described here is highly specific. While the centre of the bull's-eye is perceived to jitter, the surround

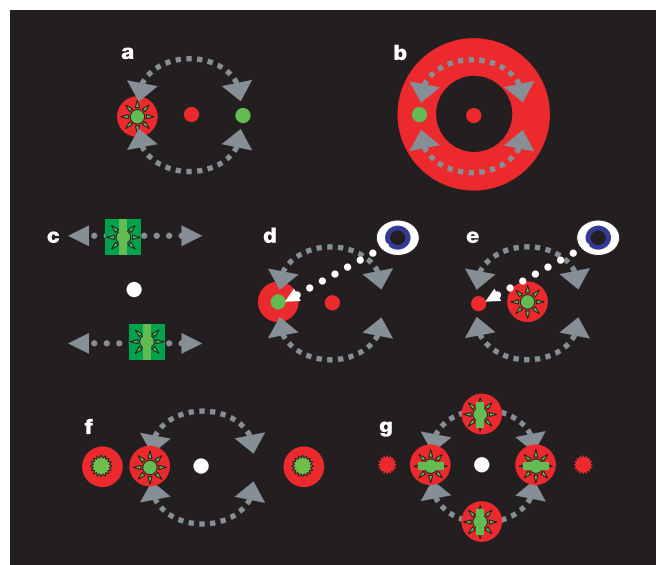


Figure 2 Schematic diagrams of the stimulus configurations. Conditions in which illusory jitter was seen are represented by starburst patterns (a, c, e–g); those in which physical flicker was shown are represented by jagged circles (f, g).

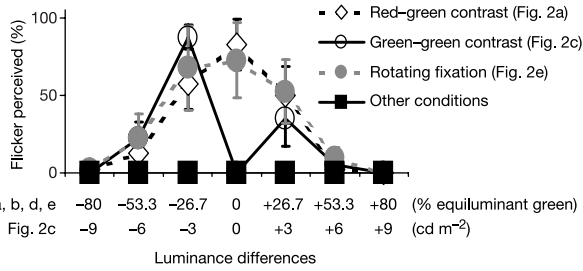


Figure 3 Perceived jitter. Percentage of times that illusory jitter was seen by four observers, naive as to the purpose of the study, as a function of the luminance difference between foreground and background regions of retinally moving stimuli (Fig. 2a, c–e) or between a rotating green dot and a red ring (Fig. 2b). For stimulus configurations shown in Fig. 2a, b, d, e, foreground luminance is expressed as a percentage ($\pm 80\%$) of green luminance perceived to match a red luminance of 18.1 cd m^{-2} , measured separately for each observer by the minimal motion method²⁰. For the configuration shown in Fig. 2c, the luminance of the central green bar was varied within a range $\pm 8.7 \text{ cd m}^{-2}$ from physical equiluminance (18.1 cd m^{-2}). Error bars show $\pm 1 \text{ s.e.m.}$

of the bull's-eye, the isolated motion and the fixation point all appear to be stable (Fig. 2a, e, f).

The illusory jitter appeared to have a characteristic rate. To estimate this rate, we constructed two stimuli in which rates of physical flicker could be matched to the perceived rate of the illusory jitter. The first consisted of three red–green bull's-eyes presented on a cathode-ray tube (CRT) monitor. One rotated around a central fixation point. The other two were static and were presented more eccentrically to the left and right of fixation (Fig. 2f). The luminance of the green centre of the rotating bull's-eye was varied. If illusory

jitter was seen, the observer introduced a sine-wave-profiled luminance flicker to the static green dots and adjusted the rate of this flicker (in steps of 5 Hz by pressing one of two response levers) until it appeared to match the rate of the illusory jitter.

To ensure that our observations were not an artefact resulting from the CRT presentation or from artificial lighting, we printed physically equiluminant red–green stimuli on a black background and rotated this image at a constant speed using an electric motor (Fig. 2g). Robust illusory jitter could be seen when this stimulus was viewed under natural daylight illumination. To estimate the rate of this jitter, we placed two light-emitting diodes (LEDs) eccentrically to the left and right of the stimulus. A pulse generator was used to create a sine-wave-profiled luminance flicker of the LEDs, and observers adjusted this rate until it seemed to match that of the illusory jitter.

Whenever illusory jitter was seen, it was reported to have a constant rate that did not vary as a function of stimulus velocity for any of our observers (Fig. 4a, c, e, g). With CRT presentation, the rate was estimated as being $\sim 25 \text{ Hz}$ (Fig. 4a, c, e). This rate did not appear to vary when the monitor refresh rate was changed (from 100 to 60 Hz). Also, from the results obtained using the CRT presentation, it was evident that the illusory jitter was seen most often when the red–green bull's-eye was at, or close to, subjective equiluminance (Fig. 4b, d, f). However, for faster and slower motions, the illusory jitter was less salient in that it was typically seen less often and over a reduced range of luminance contrasts. With the physical stimulus, the rate of illusory jitter was estimated to be $\sim 22.2 \text{ Hz}$ (Fig. 4g). If the green bars within the physical stimulus were replaced with black, no illusory jitter was ever reported.

The illusory spatial jitter has a characteristic periodicity (~ 22.2 – 25 Hz) that does not seem to vary as a function of the physical speed of the stimulus. This positional jitter cannot readily be attributed to

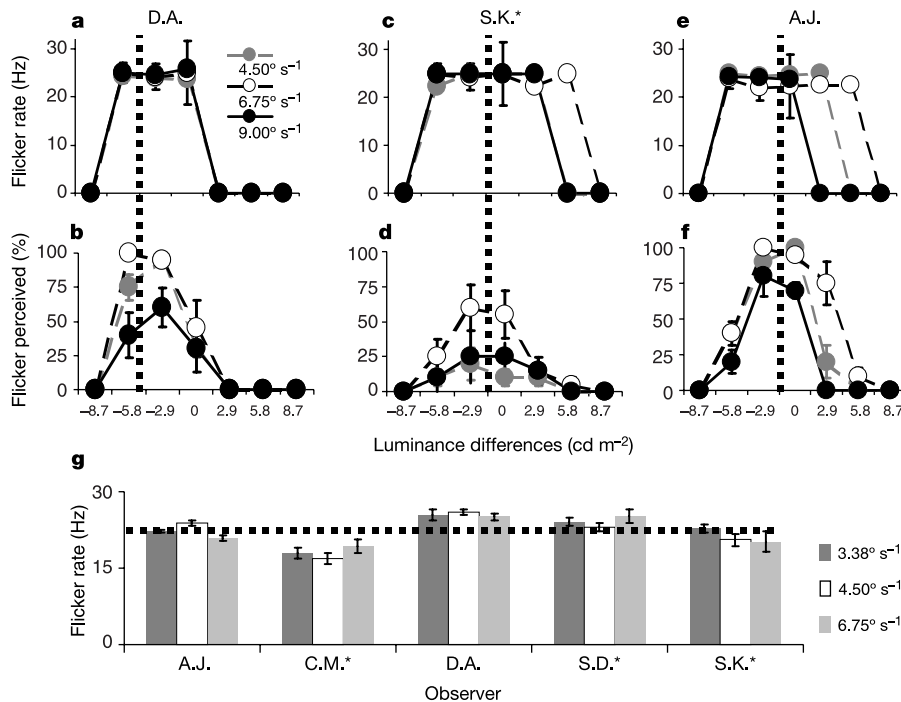


Figure 4 Perceived jitter rate. Rate (a, c, e) and percentage of times (b, d, f) that illusory jitter was seen by three observers as a function of the luminance difference between foreground (9.4 – 26.8 cd m^{-2}) and background (18.1 cd m^{-2}) regions of rotating bull's-eyes. Data for three velocities are shown. Vertical dotted lines show the foreground luminance subjectively equiluminant with the background as determined by a minimum-

motion task²⁰. g, Rate of illusory jitter within a physical sunlit stimulus for five observers as a function of stimulus velocity. The dotted horizontal line depicts the rate of perceived jitter (22.3 Hz) averaged across subjects and stimulus velocities. Error bars show $\pm 1 \text{ s.e.m.}$; asterisks placed next to the observers' initials indicate that they were naive as to the purpose of the study.

the stimulus, which is invariant in its form and motion, or to random eye movements. This leaves the possibility that it reflects a dynamic neural process. When combinations of high- and low-luminance-contrast motion are shown together, as in the examples described here, the motion cues are consistently at variance with the spatial configuration. Unless some form of resolution occurs, the two boundaries might appear to disengage⁸. We propose that the illusory jitter is a visible consequence of this resolution. It has been suggested that reciprocal feedback between, and lateral interactions within, cortical areas can cause synchronous neural spiking with a frequency in the gamma range (20–50 Hz)^{17–19}. The characteristic frequency of the illusory jitter described here might similarly reflect the temporal dynamics of recurrent neural processes that mediate the integration of motion-based spatial predictions and subsequent spatial processing. □

Methods

All stimuli used in the conditions represented in Fig. 2a–f were displayed on a 19-inch Sony Trinitron Multiscan 400PS monitor, with a refresh rate of 100 Hz, driven by a VSG 2/5 visual stimulus generator (Cambridge Research Systems). The standard configuration consisted of a large red dot (Commission Internationale d'Éclairage (CIE) 1931 chromaticity chart: $x = 0.60$, $y = 0.34$) with a diameter subtending 1.5° of visual angle, and a smaller superimposed green dot (CIE 1931: $x = 0.28$, $y = 0.595$) with a diameter subtending 0.5° . In the configurations represented in Fig. 2a, b, d–f, the rotating peripheral bull's-eyes were centred 2.25° of visual angle away from a central fixation point, and in Fig. 2f the additional locations were 3.75° eccentric. In the configuration represented in Fig. 2c, two green squares with a width and height of 1.4° were centred 2° above and below a central static fixation point. The central region had a height of 1.4° and a width of 0.25° . These stimuli were viewed in the dark from a distance of 57 cm with the head placed in a chin rest.

For all configurations, other than those depicted in Fig. 2c, g, the physical direction of motion could be clockwise or anti-clockwise, determined at random from trial to trial. During each trial in conditions Fig. 2a–f, the stimulus remained until the observer reported whether jitter was visible or not by pressing one of two levers. In these conditions, during a run of trials, seven luminance levels of the target stimulus were sampled ten times. Each data point in Fig. 3 and in Fig. 4a–f is the mean of four runs.

In the flicker-matching experiment illustrated in Fig. 2f, observers adjusted the luminance flicker frequency of peripheral dots in 5 Hz steps. Note that this sine-wave luminance function was sampled at the monitor refresh rate, 100 Hz. The physical stimulus depicted in Fig. 2g contained four red dots, with a diameter subtending 2° centred 2.25° of visual angle away from a central fixation point. Equiluminant green bars, with a height of 1.25° and a width of 0.25° , were centred within the red dots. The direction of rotation was clockwise and the orientation of the bars was orthogonal to the direction of rotation. LEDs were placed 3.75° eccentrically to the left and right of the central fixation point. Before the peripheral LEDs were shown, it was confirmed that each observer could see illusory jitter of the green bars at each of three physical speeds of rotation. Observers adjusted the rate of sine-wave flicker of the LEDs by adjusting an analogue control on a pulse generator until the rate of flicker seemed to match the rate of the illusory spatial jitter. This was done ten times for each of three stimulus velocities by each observer.

Received 3 July; accepted 24 July 2003; doi:10.1038/nature01955.

1. Anstis, S. Footsteps and inchworms: Illusions show that contrast affects apparent speed. *Perception* **30**, 785–794 (2001).
2. Blakemore, M. R. & Snowden, R. J. The effect of contrast upon perceived speed: a general phenomenon? *Perception* **28**, 33–48 (1999).
3. Cavanagh, P., Tyler, C. W. & Favreau, O. E. Perceived velocity of moving chromatic gratings. *J. Opt. Soc. Am. A* **1**, 893–899 (1984).
4. Thompson, P. Perceived rate of movement depends on contrast. *Vision Res.* **22**, 377–380 (1982).
5. De Valois, R. L. & De Valois, K. K. Vernier acuity with stationary moving Gabors. *Vision Res.* **31**, 1619–1626 (1991).
6. Nishida, S. & Johnston, A. Influence of motion signals on the perceived position of spatial pattern. *Nature* **397**, 610–612 (1999).
7. Whitney, D. & Cavanagh, P. Motion distorts visual space: shifting the perceived position of remote stationary objects. *Nature Neurosci.* **3**, 954–959 (2000).
8. Nguyen-Tri, D. & Faubert, J. The fluttering-heart illusion: a new hypothesis. *Perception* **32**, 627–634 (2003).
9. Helmholtz, H. *Treatise on Physiological Optics* (Dover, New York, 1962).
10. von Grunau, M. W. The “fluttering heart” and spatio-temporal characteristics of color processing III. Interactions between the systems of the rods and the long-wavelength cones. *Vision Res.* **16**, 397–401 (1976).
11. Bridgeman, B. & Stark, L. Ocular proprioception and efference copy in registering visual direction. *Vision Res.* **31**, 1903–1913 (1991).
12. Sherrington, C. S. Observations on the sensual role of the proprioceptive nerve supply of the extrinsic ocular muscles. *Brain* **41**, 332–343 (1918).
13. Wiesel, T. N. & Hubel, D. H. Spatial and chromatic interactions in the lateral geniculate body of the rhesus monkey. *J. Neurophysiol.* **29**, 1115–1116 (1966).
14. Campbell, F. W., Robson, J. G. & Westheimer, G. Fluctuations of accommodation under steady viewing. *J. Physiol. (Lond.)* **145**, 579–594 (1959).

15. Murakami, I. & Cavanagh, P. A jitter after-effect reveals motion-based stabilization of vision. *Nature* **395**, 798–801 (1998).
16. Murakami, I. Illusory jitter in a static stimulus surrounded by a synchronously flickering pattern. *Vision Res.* **43**, 957–969 (2003).
17. Von der Marlsburg, C. & Schneider, W. A neural cocktail-party processor. *Biol. Cybern.* **54**, 29–40 (1986).
18. Engel, A. K., Konig, P., Kreiter, A. K. & Singer, W. Interhemispheric synchronization of oscillatory neuronal responses in cat visual cortex. *Science* **252**, 1177–1179 (1991).
19. Engel, A. K. & Singer, W. Temporal binding and the neural correlates of sensory awareness. *Trends Cogn. Sci.* **5**, 16–25 (2001).
20. Anstis, S. M. & Cavanagh, P. in *Color Vision: Physiology and Psychophysics* (eds Mollon, J. D. & Sharpe, L. T.) 155–166 (Academic, London, 1983).

Supplementary Information accompanies the paper on www.nature.com/nature.

Acknowledgements We are grateful to C. Clifford, J. Dale, F. Kandil, S. Nishida and Q. Zaidi for their suggestions and comments.

Competing interests statement The authors declare that they have no competing financial interests.

Correspondence and requests for materials should be addressed to D.H.A. (derek.arnold@ucl.ac.uk).

Cellular networks underlying human spatial navigation

Arne D. Ekstrom¹, Michael J. Kahana¹, Jeremy B. Caplan¹, Tony A. Fields², Eve A. Isham², Ehren L. Newman¹ & Itzhak Fried^{2,3}

¹Volen Center for Complex Systems, Brandeis University, Waltham, Massachusetts 02454, USA

²Division of Neurosurgery and Department of Psychiatry and Biobehavioral Science, University of California, Los Angeles (UCLA), California 90095, USA

³Functional Neurosurgery Unit, Tel-Aviv Medical Center and Sackler School of Medicine, Tel-Aviv University, Tel-Aviv 69978, Israel

Place cells of the rodent hippocampus constitute one of the most striking examples of a correlation between neuronal activity and complex behaviour in mammals^{1,2}. These cells increase their firing rates when the animal traverses specific regions of its surroundings, providing a context-dependent map of the environment^{3–5}. Neuroimaging studies implicate the hippocampus and the parahippocampal region in human navigation^{6–8}. However, these regions also respond selectively to visual stimuli^{9–13}. It thus remains unclear whether rodent place coding has a homologue in humans or whether human navigation is driven by a different, visually based neural mechanism. We directly recorded from 317 neurons in the human medial temporal and frontal lobes while subjects explored and navigated a virtual town. Here we present evidence for a neural code of human spatial navigation based on cells that respond at specific spatial locations and cells that respond to views of landmarks. The former are present primarily in the hippocampus, and the latter in the parahippocampal region. Cells throughout the frontal and temporal lobes responded to the subjects' navigational goals and to conjunctions of place, goal and view.

Responses of single neurons were recorded in seven subjects who were patients with pharmacologically intractable epilepsy undergoing invasive monitoring with intracranial electrodes to identify the seizure focus for potential surgical treatment (see Methods). Subjects played a taxi driver computer game in which they explored a virtual town, searching for passengers who appeared in random spatial locations and delivering them to fixed target locations (shops, Fig. 1a, b). Before exploring the town, recordings were